

Fast Detection of a Weak Signal by a Stochastic Resonance Induced by a Coherence Resonance in an Excitable GaAs/Al_{0.45}Ga_{0.55}As Superlattice

Zhengzheng Shao,¹ Zhizhen Yin,² Helun Song,² Wei Liu,² Xiujuan Li,¹ Jubo Zhu,¹ Klaus Biermann,³
Luis L. Bonilla,⁴ Holger T. Grahn,^{3,*} and Yaohui Zhang^{1,2,†}

¹College of Liberal Arts and Sciences, National University of Defense Technology, Changsha 410073, China

²Key Laboratory of Nanodevices and Applications, Suzhou Institute of Nano-Tech and Nano-Bionics, Chinese Academy of Sciences, Suzhou 215123, China

³Paul-Drude-Institut für Festkörperelektronik, Leibniz-Institut im Forschungsverbund Berlin e. V., Hausvogteiplatz 5–7, 10117 Berlin, Germany

⁴Gregorio Millán Institute for Fluid Dynamics, Nanoscience and Industrial Mathematics, and Department of Materials Science and Engineering and Chemical Engineering, Universidad Carlos III de Madrid, 28911 Leganés, Spain



(Received 19 December 2017; published 24 August 2018)

The effect of a coherence resonance is observed experimentally in a GaAs/Al_{0.45}Ga_{0.55}As superlattice under dc bias at room temperature, which is driven by noise. For an applied voltage, for which no current self-oscillations are observed, regular current self-oscillations with a frequency of about 82 MHz are induced by exceeding a certain noise amplitude. In addition, a novel kind of a stochastic resonance is identified, which is triggered by the coherence resonance. This stochastic resonance appears when the device is driven by an external ac signal with a frequency, which is relatively close to that of the regular current self-oscillations at the coherence resonance. The intrinsic oscillation mode in the coherence resonance is found to be phase locked by an extremely weak ac signal. It is demonstrated that an excitable superlattice device can be used for the fast detection of weak signals submerged in noise. These results are very well reproduced by results using numerical simulations based on a sequential resonant tunneling model of nonlinear electron transport in semiconductor superlattices.

DOI: [10.1103/PhysRevLett.121.086806](https://doi.org/10.1103/PhysRevLett.121.086806)

Noise has been demonstrated to result in many non-linear physical systems in surprisingly constructive effects such as the coherence resonance [1–4] and the stochastic resonance [5–9]. If no external periodic driving source is present, a coherence resonance occurs, when oscillations excited by noise exhibit a maximum for a certain noise amplitude. In contrast, a stochastic resonance is present when random noise can enhance the signal-to-noise ratio of a periodically driven nonlinear system. Even though there is a vast amount of research activity on fundamental noise-induced ordering phenomena in physics, chemistry, and biology [10–12], useful applications of noise-induced phenomena in technologically relevant devices are still scarce.

A doped, weakly coupled semiconductor superlattice (SSL) is a nonlinear system with many degrees of freedom, whose effective nonlinearity originates from the well-to-well sequential resonant tunneling process. There are a number of very different spatiotemporal patterns observed in dc-biased SSLs including static high-field domains as well as self-sustained periodic and quasiperiodic current oscillations [13–15]. The current-voltage characteristics of these devices clearly exhibits multistability, which is a typical property of a nonlinear system. Doped SSLs under

dc bias have also been demonstrated to be an excitable system with a global constraint [14,15]. A coherence resonance in a SSL has been theoretically predicted [4] and subsequently experimentally observed in a GaAs/AlAs SL driven by noise at low temperatures [16]. In contrast, the observation of a stochastic resonance has not been reported so far in SSLs, neither theoretically nor experimentally. A stochastic resonance in SSLs has the potential to enhance the signal-to-noise ratio in order to detect very weak signals submerged in noise.

A few years ago, spontaneous chaotic [17,18] as well as periodic and quasiperiodic current self-oscillations [19] were observed in GaAs/Al_xGa_{1-x}As SLs at room temperature, when the Al mole fraction x in the barrier layers was chosen to be 0.45 to suppress the thermal leakage current through the X valley [20]. In this way, the effective nonlinearity is sufficiently strong so that a dc-biased GaAs/Al_{0.45}Ga_{0.55}As SL can become an excitable nonlinear dynamical system even at room temperature.

Very recently, we investigated the effect of noise on spontaneous chaotic current oscillations in a dc-biased GaAs/Al_{0.45}Ga_{0.55}As SL using noise with a bandwidth much smaller than the oscillation frequency [21]. With

increasing noise amplitude, the spontaneous chaotic current oscillations appear over a wider bias voltage range so that increased noise can enhance chaotic current oscillations in SSLs.

In this Letter, we present the first observation of a coherence resonance at room temperature in a dc-biased GaAs/Al_{0.45}Ga_{0.55}As SL driven by noise with a bandwidth larger than the oscillation frequency. In this case, the application of noise changes the SSL dynamics from static to regular current self-oscillations. The oscillation peak is located at a frequency of 82 MHz, and its frequency changes somewhat with increasing amplitude of the external noise. As the SSL is driven by both external noise and a weak ac signal with a frequency close to that of the intrinsic oscillation frequency for a coherence resonance, a stochastic resonance is identified in this SSL at room temperature. The corresponding results of numerical simulations based on a sequential resonant tunneling model of nonlinear electron transport in semiconductor superlattices are presented in Ref. [22]. The amplitude of the ac signal can be amplified by the external noise source, which demonstrates that the signal-to-noise ratio can be increased to values above 20 dB. More surprisingly, the weak external ac signal is able to phase lock to the intrinsic oscillations at the coherence resonance, even though the amplitude of the external ac signal is much smaller than the amplitude of the intrinsic current oscillation at the coherence resonance. This observation shows that this type of a SSL device may function as a resonance cavity within a certain frequency range and may be used as a weak-signal pre-amplifier with an enhanced signal-to-noise ratio.

The investigated weakly coupled GaAs/(Al,Ga)As SL consists of 50 periods using 7.0-nm-thick GaAs wells and 4.0-nm-thick Al_{0.45}Ga_{0.55}As barriers with the central 3.0 nm of each GaAs quantum well being Si doped. The detailed sample structure of the SSL is described in Ref. [18]. Square mesas with a side length of 30 μm are investigated. The experimental setup for the stochastic resonance measurements was implemented by adding an input sinusoidal signal superimposed on the noise signal via a coupler to the radio frequency port of a bias tee, which is directed to the measured SSL device as shown in the inset of Fig. 1. The white noise signal with a root mean square (rms) amplitude $V_{\text{noise}}^{\text{rms}}$ is generated by a Noisecom NC302L noise diode and amplified with a bandwidth of 1 GHz. The output impedance of the amplifier for the noise source is adjusted to 50 Ω to match that of the bias tee. The dc bias V_{dc} is supplied by a Keithley 2612A SMU. The sinusoidal ac signal with an amplitude V_{sin} was produced by the signal generator Agilent E4432B. For the experimental setup of the measurement of the coherence resonance, a 50 Ω radio frequency resistor was used to replace the ac signal source so that impedance matching was realized. The current versus time traces and the frequency spectra were recorded using the 6-GHz oscilloscope LeCroy Wavepro 760Zi-A.

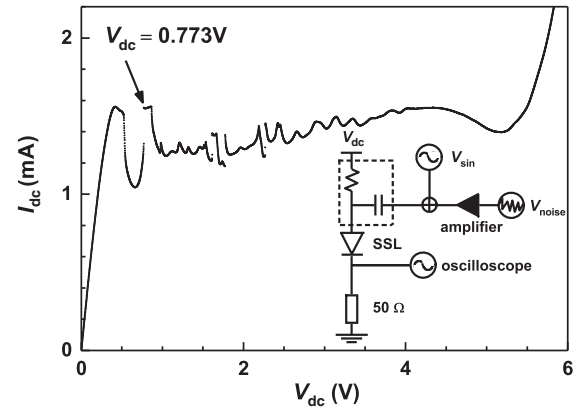


FIG. 1. Measured current-voltage ($I_{\text{dc}} - V_{\text{dc}}$) characteristics of the investigated, weakly coupled SSL for a voltage range from 0 to 6 V. Inset: Experimental setup for the measurement of a stochastic resonance. The dashed rectangle marks the bias tee. In the coherence resonance experiment, the 50 Ω radio-frequency resistor is used to replace the sinusoidal signal in order to ensure that the entire circuit is impedance matched to 50 Ω . The sinusoidal ac signal is produced using the signal generator Agilent E4432B. The white noise is produced by a Noisecom NC302L noise diode.

All experimental measurements were performed at room temperature.

Figure 1 displays the measured, time-averaged current-voltage ($I_{\text{dc}} - V_{\text{dc}}$) characteristics of the SSL device. There is a plateau region between 0.51 and 5.26 V with some variations in the current level. In this voltage range, a number of different spatiotemporal patterns are observed. For the dc voltage of 0.773 V, where the current exhibits a maximum as shown in Fig. 1, current oscillations are not detected so that the current is stationary. However, when noise is added, the SSL device biased at this voltage exhibits a coherence resonance at room temperature. In addition, a stochastic resonance was also detected at room temperature, when an ac signal was added. In the following, we will describe the observation of both types of resonances.

Figure 2 displays the resulting current self-oscillations for different values of $V_{\text{noise}}^{\text{rms}}$ at $V_{\text{dc}} = 0.773$ V. The ac components of the SSL current versus time and the corresponding frequency spectra are shown in Figs. 2(a)–2(e) and 2(f)–2(j), respectively, for different values of $V_{\text{noise}}^{\text{rms}}$ as indicated in the frequency spectra. When $V_{\text{noise}}^{\text{rms}}$ exceeds 8.287 mV, a periodic current oscillation with a fundamental frequency of about 82 MHz appears with a noisy background. As $V_{\text{noise}}^{\text{rms}}$ is increased, the frequency of the periodic oscillations increases. At the same time, the amplitude of the background noise also increases. In Fig. 2(g), the spectrum of the oscillation peak is distributed between 75 and 100 MHz. The input noise consists of white noise; i.e., the spectrum is very wide and the amplitude is constant over the whole spectrum. In contrast, after the noise is applied to the SSL device, it becomes enhanced in the spectral range of the

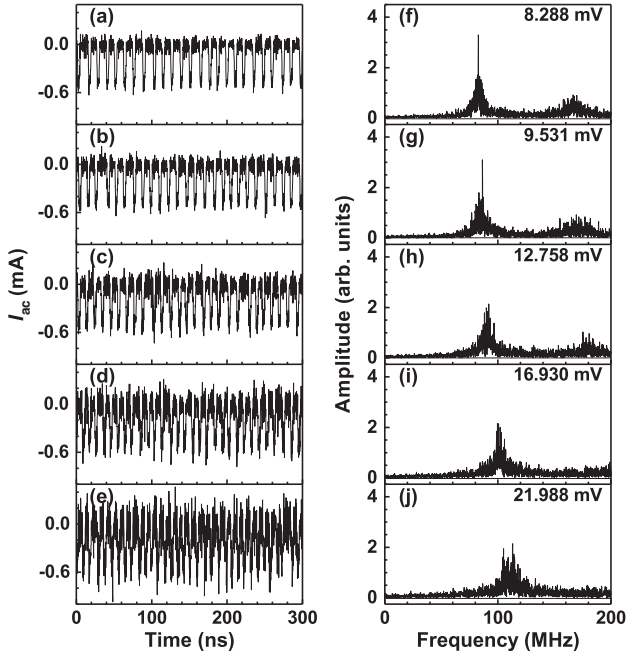


FIG. 2. (a)–(e) ac components of the SSL current I_{ac} versus time and (f)–(j) corresponding frequency spectra for different noise amplitudes at $V_{dc} = 0.773$ V. The values of V_{noise}^{rms} are (a) and (f) 8.288, (b) and (g) 9.531, (c) and (h) 12.758, (d) and (i) 16.930, as well as (e) and (j) 21.988 mV as indicated in the frequency spectra.

oscillation peak as shown, e.g., in Fig. 2(g). Therefore, we conclude that the bandwidth of the background noise, which exhibits a Gaussian distribution, is limited to about 25 MHz. The overall behavior agrees very well with the results of the numerical simulations [22].

Figure 3 shows the normalized standard deviation R_{T_a} of the interspike interval $\langle T_a \rangle$

$$R_{T_a} = \frac{\sqrt{\langle T_a^2 \rangle - \langle T_a \rangle^2}}{\langle T_a \rangle} \quad (1)$$

as a function of V_{noise}^{rms} . The quantity R_{T_a} , which is a measure of the regularity of the oscillations, is a concave function of V_{noise}^{rms} , exhibiting a minimum for intermediate values of V_{noise}^{rms} . This is the typical signature of a coherence resonance, which for the first time is experimentally observed in a solid-state device at room temperature. The appearance of the coherence resonance agrees very well with the results of the numerical simulations [22].

For values of V_{noise}^{rms} less than 8.287 mV, the current oscillations appear to be quite different. The inset of Fig. 3 displays the average values of the interspike intervals in the time domain $\langle T_a \rangle$ versus V_{noise}^{rms} . While $\langle T_a \rangle$ is almost constant with a value of about 10 ns for $V_{noise}^{rms} > 8.287$ mV, $\langle T_a \rangle$ increases by two orders of magnitude for $V_{noise}^{rms} < 8.287$ mV. According to the results of a stochastic model presented in Ref. [4], this behavior is induced by a saddle-node infinite-period bifurcation.

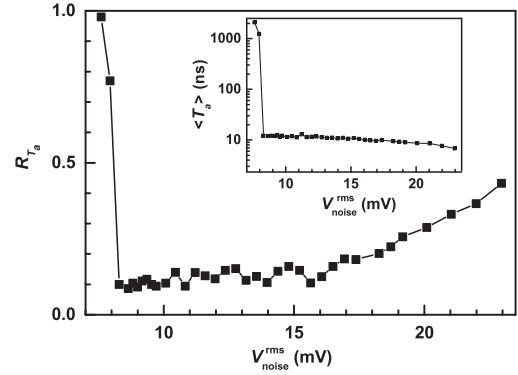


FIG. 3. Normalized standard deviation R_{T_a} versus V_{noise}^{rms} . The inset shows the mean interspike interval $\langle T_a \rangle$ versus V_{noise}^{rms} .

In addition to the dc bias and the noise, we can also add a sinusoidal ac signal with a rather small amplitude. Figures 4(a)–4(e) and 4(f)–4(j) display the ac components of the SSL current versus time and the corresponding frequency spectra, respectively, for this SSL device at $V_{dc} = 0.773$ V with an additional sinusoidal ac signal with a frequency of 76 MHz and $V_{sin} = 0.723$ mV for different values of V_{noise}^{rms} as indicated in the frequency spectra. Note that V_{sin} is about one order of magnitude smaller than V_{noise}^{rms} .

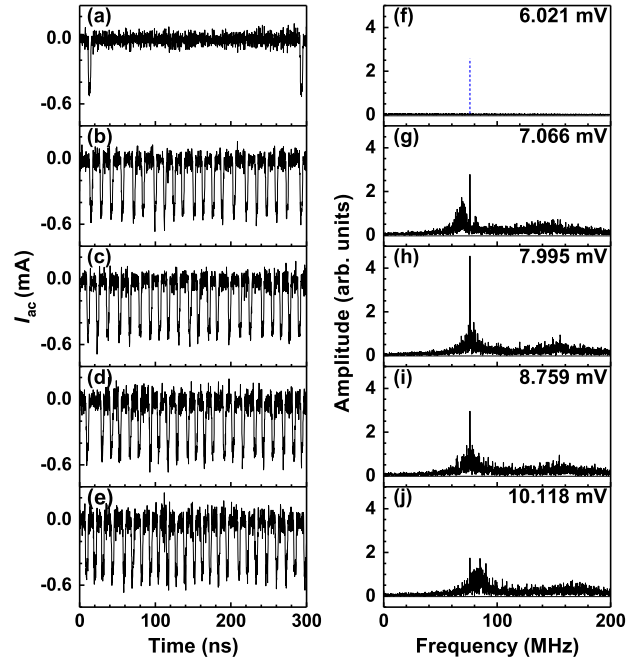


FIG. 4. (a)–(e) ac components of the SSL current I_{ac} versus time and (f)–(j) corresponding frequency spectra for different noise amplitudes at $V_{dc} = 0.773$ V as well as a sinusoidal ac signal with a frequency of 76 MHz and an amplitude $V_{sin} = 0.723$ mV. The values of V_{noise}^{rms} are (a) and (f) 6.021, (b) and (g) 7.066, (c) and (h) 7.995, (d) and (i) 8.759, as well as (e) and (j) 10.118 mV. The time window for all data acquisitions amounts to 20 μ s. In (f), the output signal is almost submerged in the noise. The dashed line corresponds to a frequency of 76 MHz.

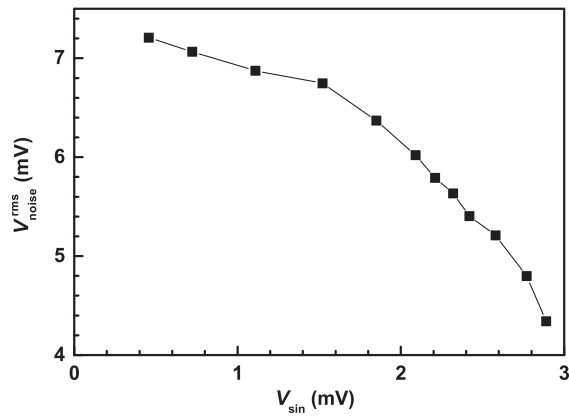


FIG. 5. Values of $V_{\text{noise}}^{\text{rms}}$ that are necessary to trigger the periodic current oscillations versus values of V_{sin} .

When $V_{\text{noise}}^{\text{rms}}$ is rather small with a value of 6.021 mV, some chaotic pulses are observed, which exhibit a very large separation in the time traces. Once $V_{\text{noise}}^{\text{rms}}$ reaches 7.066 mV, periodic current oscillations with a fundamental frequency of 76 MHz suddenly appear, which may be considered as a nonlinear amplification of the externally applied ac signal.

There are two important results present in Fig. 4. First, the periodic current oscillation mode in the coherence

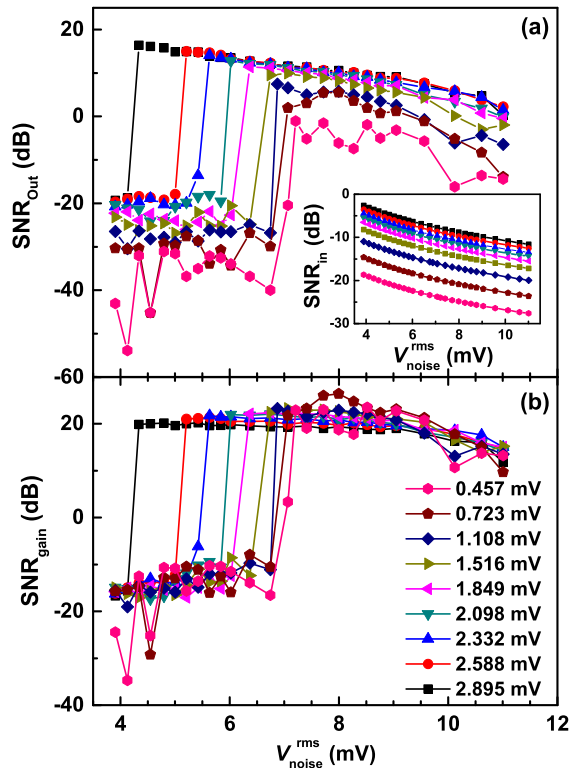


FIG. 6. (a) SNR_{out} (inset: SNR_{in}) and (b) SNR_{gain} versus $V_{\text{noise}}^{\text{rms}}$, which was varied between 3.905 and 11.008 mV. The amplitude V_{sin} was changed from 0.457 to 2.895 mV as indicated by the different colors. The input signal is fixed at 76 MHz, and the cutoff frequency of the noise is 1 GHz.

resonance configuration of Fig. 2 does not appear anymore, and only the amplified external ac signal is observed, which implies that the intrinsic coherence resonance oscillation mode with a larger amplitude can be phase locked to a weak external ac signal. Second, a smaller value of $V_{\text{noise}}^{\text{rms}}$ can already trigger periodic oscillations as compared with the values of $V_{\text{noise}}^{\text{rms}}$ in the coherence resonance configuration of Fig. 2. The ac signal appears to be more effective in inducing current self-oscillations than the noise.

Figure 5 shows the values of $V_{\text{noise}}^{\text{rms}}$ that are necessary to trigger the periodic current oscillations as a function of V_{sin} . The larger V_{sin} , the smaller the value of $V_{\text{noise}}^{\text{rms}}$ for triggering periodic current oscillations. However, the sum of these two amplitudes is not constant as can be seen from Fig. 5, since $V_{\text{noise}}^{\text{rms}}$ for triggering periodic current oscillations versus V_{sin} is not a straight line.

As $V_{\text{noise}}^{\text{rms}}$ is increased, the amplitude of the 76-MHz current self-oscillations first increases and then decreases. This behavior is more clearly visible in the frequency spectra shown in Figs. 4(f)–4(j) and has the signature of a stochastic resonance, which is demonstrated experimentally in an excitable SSL system for the first time. The experimental observations are well reproduced by the results of the numerical simulations [22].

Figures 6(a) and 6(b) display the output signal-to-noise ratio $\text{SNR}_{\text{out}} = V_{\text{signal}}/V_{\text{noise}}^{\text{rms}}$, where V_{signal} refers to the voltage amplitude of the current oscillations in Fig. 4, and the gain of the signal-to-noise ratio $\text{SNR}_{\text{gain}} = \text{SNR}_{\text{out}}/\text{SNR}_{\text{in}}$ of the SSL device in the stochastic resonance configuration, respectively. The experimental data in this figure clearly demonstrate the main features of a stochastic resonance in an excitable SSL at room temperature. The value of $V_{\text{noise}}^{\text{rms}}$ to trigger the stochastic resonance is strongly correlated with the value of V_{sin} . The stochastic resonance in the SSL device can result in an enhancement of the signal-to-noise ratio by more than 30 dB (more than 100 dB in the

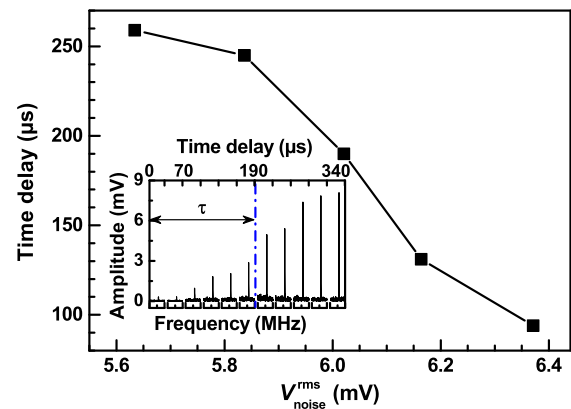


FIG. 7. Time delay τ versus $V_{\text{noise}}^{\text{rms}}$. The inset displays the spectra of the output signals for multiple time intervals at $V_{\text{noise}}^{\text{rms}} = 6.021$ mV. The spectra peak at 76 MHz, which is the same as the frequency of the input signal.

results of the numerical simulations [22]) so that an ac signal with a much smaller amplitude than the background noise can be detected. This observation may result in a different way to amplify weak ac signals by using excitable SSL devices. The method of operation is similar to a lock-in amplifier that is typically used for amplifying and detecting weak ac signals submerged in strong background noise.

The response of a stochastic resonance in an excitable SSL was measured with an externally applied noise signal as shown in Fig. 7. The time delay was extracted as displayed in the inset of Fig. 7. The response time of the stochastic resonance amounts to less than half a millisecond. Thus, the stochastic resonance in a SSL devices has the advantage that a weak ac signal can be detected very fast as compared to lock-in amplifiers, whose typical response times are in the range of tens of milliseconds.

In conclusion, we have experimentally observed a coherence resonance as well as a stochastic resonance in a weakly coupled GaAs/Al_{0.45}Ga_{0.55}As SL at room temperature. The stochastic resonance appears as a result of the coherence resonance, when the frequency of the externally applied ac signal falls into the frequency range of the coherence resonance. In this case, the intrinsic oscillation modes of the coherence resonance can be phase locked by the externally applied weak ac signal. All these results are in very good qualitative agreement with the results of the numerical simulations [22]. Thus, the stochastic resonance in excitable SSL devices can be used as a lock-in amplifier, but with a much smaller integration time than available for conventional lock-in amplifiers.

The authors would like to thank M. Carretero, E. Mompo, and S. W. Teitsworth for technical support and fruitful discussions. The authors would also like to thank the Strategic Leading Science and Technology Special Program of the Chinese Academy of Sciences (Grant No. XDA06010705), the National Natural Science Foundation of China (Grants No. 61070040 and No. 61204093), the National Key Research and Development Program of China (Grant No. 2016YFE0129400), the Exploration Project (Grant No. 7131266), and the Ministerio de Economía y Competitividad of Spain (Grants No. MTM2014-56948-C2-2-P and No. MTM2017-84446-C2-2-R) for financial support.

Z. S. and Z. Y. contributed equally to this work.

*htgrahn@pdi-berlin.de

†yh Zhang2006@sinano.ac.cn

- [1] A. S. Pikovsky and J. Kurths, *Phys. Rev. Lett.* **78**, 775 (1997).
- [2] G. Giacomelli, M. Giudici, S. Balle, and J. R. Tredicce, *Phys. Rev. Lett.* **84**, 3298 (2000).
- [3] J. F. Martinez Avila, H. L. D. de S. Cavalcante, and J. R. Rios Leite, *Phys. Rev. Lett.* **93**, 144101 (2004).
- [4] J. Hizanidis, A. Balanov, A. Amann, and E. Schöll, *Phys. Rev. Lett.* **96**, 244104 (2006).
- [5] S. Fauve and F. Heslot, *Phys. Lett. A* **97**, 5 (1983).
- [6] B. McNamara, K. Wiesenfeld, and R. Roy, *Phys. Rev. Lett.* **60**, 2626 (1988).
- [7] R. Löfstedt and S. N. Coppersmith, *Phys. Rev. Lett.* **72**, 1947 (1994).
- [8] G. J. Escalera Santos, M. Rivera, and P. Parmananda, *Phys. Rev. Lett.* **92**, 230601 (2004).
- [9] H. Abbaspour, S. Trebaol, F. Morier-Genoud, M. T. Portella-Oberli, and B. Deveaud, *Phys. Rev. Lett.* **113**, 057401 (2014).
- [10] J. K. Douglass, L. Wilkens, E. Pantazelou, and F. Moss, *Nature (London)* **365**, 337 (1993).
- [11] D. S. Leonard and L. E. Reichl, *Phys. Rev. E* **49**, 1734 (1994).
- [12] P. Hänggi, *ChemPhysChem* **3**, 285 (2002).
- [13] J. Kastrop, R. Klann, H. T. Grahn, K. Ploog, L. L. Bonilla, J. Galán, M. Kindelan, M. Moscoso, and R. Merlin, *Phys. Rev. B* **52**, 13761 (1995).
- [14] L. L. Bonilla, *J. Phys. Condens. Matter* **14**, R341 (2002).
- [15] L. L. Bonilla and H. T. Grahn, *Rep. Prog. Phys.* **68**, 577 (2005).
- [16] Y. Y. Huang, H. Qin, W. Li, S. L. Lu, J. R. Dong, H. T. Grahn, and Y. H. Zhang, *Europhys. Lett.* **105**, 47005 (2014).
- [17] Y. Y. Huang, W. Li, W. Q. Ma, H. Qin, and Y. H. Zhang, *Chin. Sci. Bull.* **57**, 2070 (2012).
- [18] W. Li, I. Reidler, Y. Aviad, Y. Y. Huang, H. Song, Y. H. Zhang, M. Rosenbluh, and I. Kanter, *Phys. Rev. Lett.* **111**, 044102 (2013).
- [19] Y. Y. Huang, W. Li, W. Q. Ma, H. Qin, H. T. Grahn, and Y. H. Zhang, *Appl. Phys. Lett.* **102**, 242107 (2013).
- [20] J. B. Xia, *Phys. Rev. B* **41**, 3117 (1990).
- [21] Z. Z. Yin, H. Song, Y. H. Zhang, M. Ruiz-García, M. Carretero, L. L. Bonilla, K. Biermann, and H. T. Grahn, *Phys. Rev. E* **95**, 012218 (2017).
- [22] E. Mompo, M. Ruiz-García, M. Carretero, H. T. Grahn, Y. H. Zhang, and L. L. Bonilla, *Phys. Rev. Lett.*, preceding Letter, **121**, 086805 (2018).